High accuracy ^{234}U(n,f) cross section in the resonance energy region

E. Leal-Cidoncha[1,a], I. Durán[1], C. Paradela[1,31], L. Tassan-Got[2], L. Audouin[2], L.C. Leal[3], C. Le Naour[2], G. Noguere[4], D. Tarrío[1,33], L.S. Leong[2], S. Altstadt[5], J. Andrzejewski[6], M. Barbagallo[7], V. Bécares[8], F. Bečvář[9], F. Belloni[31], E. Berthoumieux[10], J. Billowes[12], V. Boccone[11], D. Bosnar[13], M. Brugger[11], M. Calviani[11], F. Calviño[14], D. Cano-Ott[8], C. Carrapiço[15], F. Cerutti[11], E. Chiaveri[11], M. Chin[11], N. Colonna[7], G. Cortés[14], M.A. Cortés-Giraldo[16], M. Diakaki[10], C. Domingo-Pardo[18], R. Dressler[19], C. Eleftheriadis[21], A. Ferrari[11], K. Fraval[10], S. Ganesan[22], A.R. García[8], G. Giubrone[18], M.B. Gómez-Hornillos[14], I.F. Gonçalves[15], E. González-Romero[8], E. Griesmayer[23], C. Guerrero[16], F. Gunsing[10], P. Gurusamy[22], A. Hernández-Prieto[11], D.G. Jenkins[24], E. Jericha[23], Y. Kadi[11], F. Käppeler[25], D. Karadimos[17], N. Kivel[19], M. Kokkoris[17], M. Krtička[9], J. Kroll[9], C. Lampoudis[21], C. Langer[5], C. Lederer[5,26], H. Leeb[23], R. Losito[11], A. Mallick[22], A. Manousos[21], J. Marganiec[6], T. Martínez[8], C. Massimi[27], P.F. Mastinu[20], M. Mastromarco[7], M. Meaze[7], E. Mendoza[8], A. Mengoni[28], P.M. Milazzo[29], F. Mingrone[27], M. Mirea[30], W. Mondelaers[31], A. Pavlik[26], J. Perkowski[6], A. Plompen[31], J. Praena[34], J.M. Quesada[16], T. Rauscher[35,32], R. Reifarth[5], A. Riego[14], M.S. Robles[1], F. Roman[11], C. Rubbia[11], M. Sabaté-Gilarte[11,16], R. Sarmento[15], A. Saxena[22], P. Schillebeeckx[31], S. Schmidt[5], D. Schumann[19], G. Tagliente[7], J.L. Tain[18], A. Tsinganis[11], S. Valenta[9], G. Vannini[27], V. Variale[7], P. Vaz[15], A. Ventura[28], R. Versaci[11], M.J. Vermeulen[24], V. Vlachoudis[11], R. Vlastou[17], A. Wallner[36], T. Ware[12], M. Weigand[5], C. Weiß[11], T. Wright[12], P. Žugec[13], and the n_TOF Collaboration

[1] Universidade de Santiago de Compostela (USC), Spain
[2] Centre National de la Recherche Scientifique/IN2P3 - IPN, Orsay, France
[3] IRSN/PSN-EXP, Fontenay-aux-Roses, France
[4] CEA, Cadarache, France
[5] Johann-Wolfgang-Goethe Universität, Frankfurt, Germany
[6] Uniwersytet Lódzki, Lodz, Poland
[7] Istituto Nazionale di Fisica Nucleare, Bari, Italy
[8] Centro de Investigaciones Energeticas Medioambientales y Tecnológicas (CIEMAT), Madrid, Spain
[9] Charles University, Prague, Czech Republic
[10] Commissariat à l'Énergie Atomique (CEA) Saclay - Irfu, Gif-sur-Yvette, France
[11] European Organization for Nuclear Research (CERN), Geneva, Switzerland
[12] University of Manchester, Oxford Road, Manchester, UK
[13] Department of Physics, Faculty of Science, University of Zagreb, Croatia
[14] Universitat Politecnica de Catalunya, Barcelona, Spain
[15] Instituto Tecnológico e Nuclear, Instituto Superior Técnico, Universidade Técnica de Lisboa, Lisboa, Portugal
[16] Universidad de Sevilla, Spain
[17] National Technical University of Athens (NTUA), Greece
[18] Instituto de Física Corpuscular, CSIC-Universidad de Valencia, Spain
[19] Paul Scherrer Institut, Villigen PSI, Switzerland
[20] Istituto Nazionale di Fisica Nucleare, Laboratori Nazionali di Legnaro, Italy
[21] Aristotle University of Thessaloniki, Thessaloniki, Greece
[22] Bhabha Atomic Research Centre (BARC), Mumbai, India
[23] Atominstitut, Technische Universität Wien, Austria
[24] University of York, Heslington, York, UK
[25] Karlsruhe Institute of Technology, Campus Nord, Institut für Kernphysik, Karlsruhe, Germany
[26] University of Vienna, Faculty of Physics, Austria
[27] Dipartimento di Fisica, Università di Bologna, and Sezione INFN di Bologna, Italy
[28] Agenzia nazionale per le nuove tecnologie, l'energia e lo sviluppo economico sostenibile (ENEA), Bologna, Italy
[29] Istituto Nazionale di Fisica Nucleare, Trieste, Italy
[30] Horia Hulubei National Institute of Physics and Nuclear Engineering - IFIN HH, Bucharest, Magurele, Romania
[31] European Commission JRC, Institute for Reference Materials and Measurements, Retieseweg 111, 2440 Geel, Belgium
[32] Department of Physics and Astronomy, University of Basel, Basel, Switzerland
[33] Department of Physics and Astronomy, Uppsala University, Sweden
[34] Universidad de Granada (UGRAN), Spain

e-mail: esther.leal@usc.es

[35] Centre for Astrophysics Research, School of Physics, Astronomy, Mathematics, University of Hertfordshire, UK
[36] Research School of Physics and Engineering, Australian National University, Australia

Abstract. New results are presented of the ^{234}U neutron-induced fission cross section, obtained with high accuracy in the resonance region by means of two methods using the ^{235}U(n,f) as reference. The recent evaluation of the ^{235}U(n,f) obtained with SAMMY by L. C. Leal et al. (these Proceedings), based on previous n_TOF data [1], has been used to calculate the ^{234}U(n,f) cross section through the ^{234}U/^{235}U ratio, being here compared with the results obtained by using the n_TOF neutron flux.

1. Introduction

The ^{234}U isotope is present in the uranium-enriched fuel of current reactors and is also produced during the thorium-fuel cycle. Because of its relatively low (n,f) cross section, data found in current nuclear databases could be sufficient for a first evaluation of critical reactors as well as for Accelerator Driven Systems. Nevertheless, a detailed assessment of relevant integral reactor quantities requires a more precise and complete set of basic nuclear data for this important isotope. Experimental datasets available in EXFOR as well as data in the evaluated libraries [2] show discrepancies. The ENDF/B-VII.1 and JENDL-4.0 evaluations are shifted in energy and some resonances are missing in one of the two databases. In the Resolved Resonance Region (RRR), both evaluations are based on the experimental data of James et al. [3], but JENDL-4.0 includes also the resonance parameters provided by Dridi et al. [4] for the capture reaction and the fission cross section of Heyse et al. [5] for the 5.17 eV resonance. Above 1.5 keV, in the Unresolved Resonance Region (URR), the fission data of James et al. and the capture data of Pennington were used in ENDF/B-VII.1 whereas JENDL-4.0 used the experimental data sets mentioned in Ref. [2]. The ^{234}U(n,f) cross section data presented in this work, in the neutron energy range from 3 eV up to 10 MeV, have been measured at the Neutron Time-of-Flight (n_TOF) facility at CERN with an improved detection setup based on Parallel Plate Avalanche Counters (PPACs).

2. The experimental setup

The ^{234}U(n,f) cross section was measured in 2012 during the so-called Phase-II at the CERN-n_TOF facility [6] using ten PPACs consisting of one central anode with a very fast signal (time resolution ~500 ps) and two segmented cathodes, used to measure the two coordinates of the fission fragment (FF) hit [7]. The targets, which consisted of thin radioactive layers electrodeposited on an aluminium foil, were interleaved with ten PPAC detectors. The data here presented correspond to three ^{234}U and two ^{235}U targets. The thickness of the Al backing was 2.0 μm for the ^{234}U and one ^{235}U and 0.7 μm for the second ^{235}U target. There was a slight isotopic contamination in the ^{235}U targets of ^{234}U (0.74%), ^{236}U (0.27%) and ^{238}U (6.28%), as well as a ^{235}U (0.077%) content in the ^{234}U targets, which has been subtracted during the data analysis.

The n_TOF spallation target in previous PPAC experiments, performed during the Phase-I [1,8] used normal water as the neutron moderator, which was changed to borated water in the last campaign of Phase-II when the data presented in this work have been taken. Important differences in the neutron flux are observed below hundreds of eV depending on the type of moderator material [9].

The PPAC configuration was also modified in Phase-II. The detectors and targets were tilted by 45° with respect to the neutron beam direction in order to reach up to 90° angular acceptance of the FF detection compared to the 60° achieved with the perpendicular setup used in Phase-I, see Ref. [7] for details.

3. Data analysis and results

The fission cross section (σ) is related to the number of detected fission events (C) per unit of incident neutron energy (E_n) by:

$$C(E_n)_x = \sigma(E_n)_x \cdot \Phi(E_n) \cdot N_x \cdot \epsilon \qquad (1)$$

where Φ is the neutron fluence, ϵ is the detection efficiency and N is the areal density of a target (x) of radius R.

3.1. ^{235}U(n,f) cross section

As the neutron fluence received by the targets during the experiment is not accurately known, the ^{235}U(n,f) has been used as a reference in the ^{234}U(n,f) cross section calculation. However, the n_TOF neutron flux shape was known [10] and was normalised with Eq. (1) using the ^{235}U(n,f) cross section area of 246.4 ± 1.2 b · eV given by the IAEA in the neutron energy interval from 7.8 to 11 eV as explained in Ref. [1].

The ^{235}U(n,f) cross section, obtained as the mean value of both ^{235}U targets, is compared in Fig. 1 with the recent evaluation presented in this conference by L. C. Leal et al., based on the data of Paradela et al. [1], and with the ENDF/B-VII.1 database. The averaged integral cross sections, calculated with the Analysis of Geel Spectrum (AGS) code [11], are provided in Table 1 where the ratios of the n_TOF data to those in each column are given in parentheses for different energy regions.

3.2. ^{234}U(n,f) cross section

The ^{234}U(n,f) cross section is calculated in this work by means of two methods, both based on the fact that all targets receive the same neutron flux and assuming that the efficiency of all detectors is the same within the uncertainties we are dealing with. With the **first method** (**n_TOF$_1$**), the ^{235}U(n,f) cross section obtained in the previous subsection has been used as a reference. The normalisation factor is inversely proportional to $N_5 \cdot \epsilon$ so, assuming that the efficiency is the same for all detectors, we can get the ^{234}U(n,f) cross section via the relation between the areal densities of the samples given by:

$$N_4 = N_5 \cdot \frac{m_4 \cdot M_5}{m_5 \cdot M_4} \qquad (2)$$

Table 1. ^{235}U(n,f) averaged integral cross sections.

E_n [eV]	n_TOF [b]	Paradela [b]	Leal [b]	IAEA [b]	ENDF/B-VII.1 [b]
100–200	21.13	21.31(0.99)	21.02(1.01)	21.17(1.00)	20.32(1.04)
200–300	20.70	20.82(0.99)	20.77(1.00)	20.69(1.00)	20.60(1.01)
300–400	13.02	12.90(1.01)	13.22(0.99)	13.14(0.99)	12.81(1.02)
400–500	13.66	13.68(1.00)	13.49(1.01)	13.78(0.99)	13.29(1.03)
500–600	15.51	15.30(1.01)	15.20(1.02)	15.17(1.02)	14.87(1.04)
600–700	11.50	11.56(1.00)	11.53(1.00)	11.51(1.00)	11.24(1.02)
700–800	11.12	11.05(1.01)	11.10(1.00)	11.10(1.00)	10.88(1.02)
800–900	8.236	8.305(0.99)	8.150(1.01)	8.213(1.00)	7.977(1.03)
900–1000	7.440	7.529(0.99)	7.370(1.01)	7.502(0.99)	7.240(1.03)
1000–2000	7.359	7.318(1.01)	7.290(1.01)	7.303(1.01)	7.138(1.03)
2000–3000	5.390	5.237(1.03)	5.330(1.01)	5.386(1.00)	5.290(1.02)
3000–4000	4.758	4.740(1.00)	4.790(0.99)	4.784(0.99)	4.778(1.00)
4000–5000	4.250	4.216(1.01)	4.270(1.00)	4.261(1.00)	4.207(1.01)
5000–6000	3.745	3.808(0.98)	3.820(0.98)	3.838(0.98)	3.905(0.96)
6000–7000	3.374	3.214(1.05)	3.350(1.01)	3.291(1.03)	3.287(1.03)
7000–8000	3.203	3.140(1.02)	3.210(1.00)	3.236(0.99)	3.158(1.01)
8000–9000	2.916	2.934(0.99)	3.090(0.94)	3.009(0.97)	2.940(0.99)
9000–10000	3.072	3.071(1.00)	3.060(1.00)	3.120(0.98)	3.043(1.01)

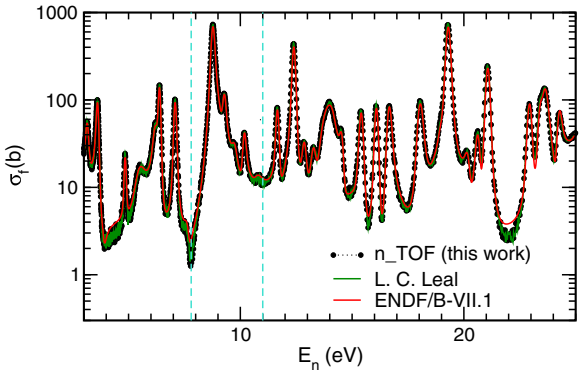

Figure 1. ^{235}U(n,f) cross section data. The dashed vertical lines correspond to the normalisation limits.

The **second method** (**n_TOF$_2$**) is based on the ratio of the number of fission events obtained for the ^{234}U and ^{235}U samples, using the ^{235}U(n,f) cross section evaluated by L.C. Leal et al., with Eq. (1), where the neutron flux and the efficiency cancel.

The cross section obtained by the first method is compared in Fig. 2 with the experimental data provided by EXFOR and with the ENDF/B-VII.1 and JENDL-4.0 evaluations. The data presented in this work have better resolution than the others, being closer to the previous n_TOF data measured by Paradela et al. [8]. A slight energy offset is observed between the ENDF/B-VII.1 and JENDL-4.0 evaluations in addition to differences in the cross sections. This energy shift is also observed between the evaluations and the experimental data, being more pronounced in the case of the JENDL-4.0 database.

Above the RRR some groups of fission resonances are observed in the experimental data, which are not evaluated in the databases, as can be seen in Fig. 3.

The averaged integral cross sections calculated with both methods are given in Table 2 for different energy regions, compared with Paradela et al., ENDF/B-VII.1 and JENDL-4.0. The ratios of the first column data over the values in the other columns are given in parentheses. On

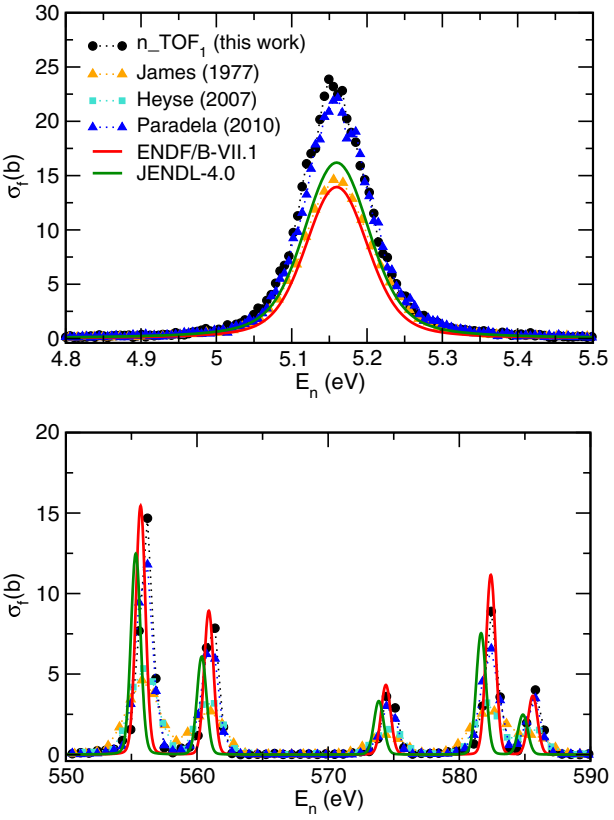

Figure 2. ^{234}U(n,f) cross section data in different energies of the RRR.

average, the differences between n_TOF$_1$ and the other columns in Table 2 are respectively 0.9% (n_TOF$_2$), −18% (Paradela), −76% (ENDF/B-VII.1) and −73% (JENDL-4.0).

3.3. Conclusions

The ^{234}U(n,f) cross section data has been obtained by means of two approaches, being in very nice agreement between them. When comparing these data with the

Table 2. ^{234}U(n,f) averaged integral cross sections.

E_n [eV]	n_TOF$_1$ [mb]	n_TOF$_2$ [mb]	Paradela [mb]	ENDF/B-VII.1 [mb]	JENDL-4.0 [mb]
100–120	365.8	343.9(1.06)	344.2(1.06)	255.0(1.43)	243.1(1.51)
120–160	26.82	26.65(1.01)	20.08(1.34)	12.81(2.09)	12.34(2.17)
160–220	80.79	79.33(1.02)	74.80(1.08)	55.08(1.47)	52.80(1.53)
220–300	61.69	60.00(1.03)	46.08(1.34)	35.98(1.71)	27.01(2.28)
300–400	84.45	77.81(1.09)	76.33(1.11)	55.92(1.51)	41.95(2.01)
400–520	486.3	490.7(0.99)	458.2(1.06)	338.5(1.44)	244.7(1.99)
520–660	498.9	507.3(0.98)	473.9(1.05)	367.2(1.36)	268.1(1.86)
660–820	153.3	164.2(0.93)	142.6(1.08)	103.5(1.48)	74.14(2.07)
820–1000	32.92	34.28(0.96)	26.26(1.25)	19.98(1.65)	15.63(2.11)
1000–1200	28.71	29.93(0.96)	22.11(1.30)	13.23(2.17)	5.858(4.90)
1200–1600	22.36	22.99(0.97)	17.01(1.31)	11.57(1.93)	9.282(2.41)
1600–2200	8.131	8.112(1.00)	5.996(1.36)	5.597(1.45)	5.486(1.48)
2200–3000	7.908	7.721(1.02)	5.201(1.52)	3.873(2.04)	9.862(0.80)
3000–4000	12.42	12.43(1.00)	9.068(1.37)	6.887(1.80)	9.757(1.27)
4000–5200	25.55	26.59(0.96)	21.02(1.22)	8.661(2.95)	12.78(2.00)
5200–6600	8.379	9.204(0.91)	8.335(1.01)	10.63(0.79)	10.56(0.79)
6600–8200	54.02	55.04(0.98)	57.33(0.94)	12.83(4.21)	25.54(2.12)
8200–10000	6.113	6.404(0.95)	7.013(0.87)	13.23(0.46)	11.99(0.51)

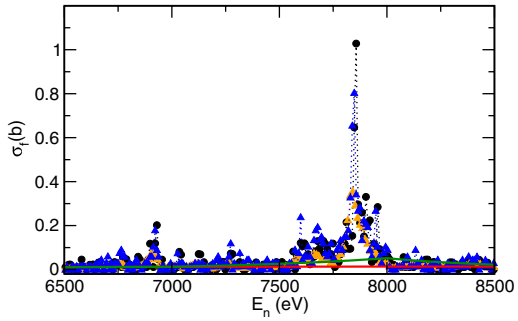

Figure 3. ^{234}U(n,f) cross section data in the 7 keV energy region.

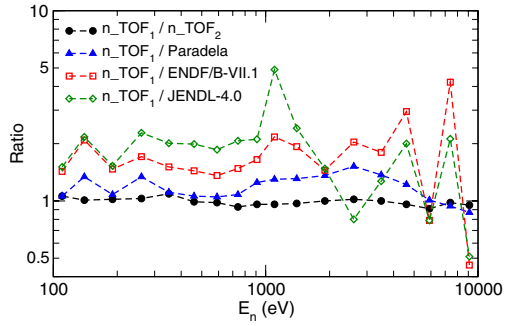

Figure 4. Ratio of the ^{234}U(n,f) integral cross sections averaged over the energy ranges given in Table 2.

experimental data provided by EXFOR, a better resolution is observed in the present data, having a shape very close to the previous n_TOF data in [8]. Huge discrepancies have been found in the cross sections and energies with the evaluations in the ENDF/B-VII.1 and JENDL-4.0 libraries.

The averaged integral cross section ratios given in parentheses in Table 2 are shown in Fig. 4, differing by factors of 0.5 to 5. It is worth to mention the good agreement between both experimental methods, the difference of −18% with respect to Paradela et al. [8] and the severe disagreement with the evaluated libraries.

References

[1] C. Paradela et al., The EPJ Conferences **111**, 02003 (2016)
[2] `www-nds.iaea.org`
[3] G.D. James et al., Phys. Rev. C **15**, 2083 (1977)
[4] W. Dridi, *PhD. Thesis* (CEA/Saclay) (2006)
[5] J. Heyse et al., Nucl. Sci. Eng. **156**, 211 (2007)
[6] F. Gunsing et al., CERN-Proceedings-2015-001, cds.cern.ch/record/2115398
[7] D. Tarrío et al., Nucl. Instrum. Meth. A **743**, 79 (2014)
[8] C. Paradela et al., Phys. Rev. C **82**, 034601 (2010)
[9] M. Barbagallo et al., EPJ A **49**(12), 1–11 (2013)
[10] n_TOF internal communication
[11] B. Becker et al., *Data reduction and uncertainty propagation of time-of-flight spectra with AGS* J. of Instrumentation **7**, P11002-19 (2012)